MACHINE INDUCED BACKGROUND IN THE LOW LUMINOSITY INSERTIONS OF THE LHC

I.Azhgirey, I.Baishev, V.Talanov*, IHEP, Protvino, Russia
K.M.Potter, CERN, Geneva, Switzerland

Abstract

The effect of the machine induced background is studied for the low luminosity insertions of the LHC. Estimations for the fluxes of the secondary particles, induced by the proton losses in the LHC, are presented for several running conditions of the collider. The formation of the background in the machine structure is discussed.

1 INTRODUCTION

Fluxes of the secondary particles, induced by proton losses upstream and downstream of the interaction points, affect the radiation environment in the corresponding insertion regions and can contribute to the detector backgrounds [1]. The characteristic feature of these secondary fluxes, or *machine induced background*, is that its value is proportional to the machine beam current, while the particle fluxes, produced in the proton-proton collisions, scale with the luminosity at a particular interaction point. This means that the relative effect of the machine induced background depends on the machine operating conditions and is different for different run scenarios.

The LHC project [2] has two insertion regions (IRs) with relatively low luminosity of proton-proton interactions, IR2 and IR8. Each IR consists of the straight section around the interaction point (IP) and two dispersion suppressors, upstream and downstream of IP. One half of the straight section, both in the IR2 and IR8, houses the injection equipment together with the appropriate injection shielding, and we present below the results of the machine background analysis for this particular part, basing on the IR2 optics structure.

2 ORIGINS OF MACHINE BACKGROUND

Secondary particle cascades can be initiated in the insertion region due to different physical processes. The generic proton losses are the interactions of the beam protons with residual gas nuclei, resulting in multiple production of secondary particles. Their distribution along the machine thus reflects the distribution of the residual gas pressure. These interactions can be divided into two types, inelastic and elastic. The secondaries from inelastic interactions have in general a resulting momentum significantly smaller than the beam particles, and can not be transported through the magnetic structure of the machine. In the arcs and dispersion suppressors, being enclosed by the machine tunnel, these particles are stopped due to the curvature of the accelerator ring and affect the radiation field mainly in the regions close to the point of the original collision. In contrast to this, secondaries produced in elastic interactions have a different behaviour. Elastic collisions of beam particles with the residual gas nuclei give in the final state energetic protons with a momentum much closer to the initial one. These *quasi–beam* particles can successfully travel with the beam long distances through the lattice to interact with the machine equipment far from the point of the primary collision [3].

3 THE CHOICE OF THE STUDIED MACHINE LENGTH

The choice of the machine length which is necessary to introduce in the simulation of the background, induced by proton losses, as well as how to account for different origins of this background, depends on the position of the studied region in the machine structure. The values of the residual gas densities determine the rate of the beam protons losses in a particular section of the machine and thus the absolute values of the machine induced background. Recently numbers became available for the H_2 equivalent average gas density in the vacuum chamber of the LHC IRs, together with the residual gas composition in the cryogenic and room temperature vacuum chambers [4]. The given numbers can be compared with the previously published data on the residual gas composition [5], taking into account the already estimated values for the machine background, induced by the proton losses in the arc cell, dispersion suppressor and straight section of IR8 [6]. This allows one to conclude that limiting the studied region to the straight section part of the insertion region will be sufficient to estimate the values of the secondary fluxes, induced by the beam–gas interaction, for the low luminosity insertion case.

4 PARTICLE CASCADE SIMULATION

Interactions of the beam protons with the nucleus of the residual gas in the straight section and the transport of the secondary cascades were simulated by the IHEP MARS program [7]. An overall threshold of 20 MeV on the particle kinetic energy was applied to the simulation of the transport for both hadrons and muons. Secondary particles were transported along the straight section up to the scoring

* talanov@mx.ihep.su

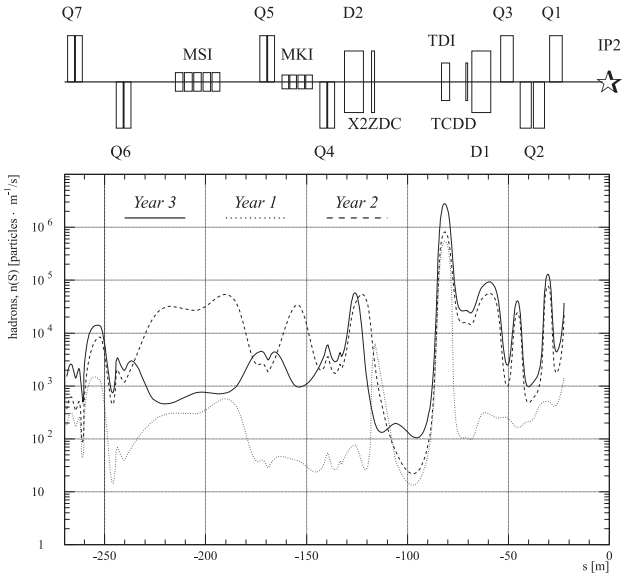

Figure 1: Number of hadrons as a function of primary proton-nucleus interaction distance to IP2.

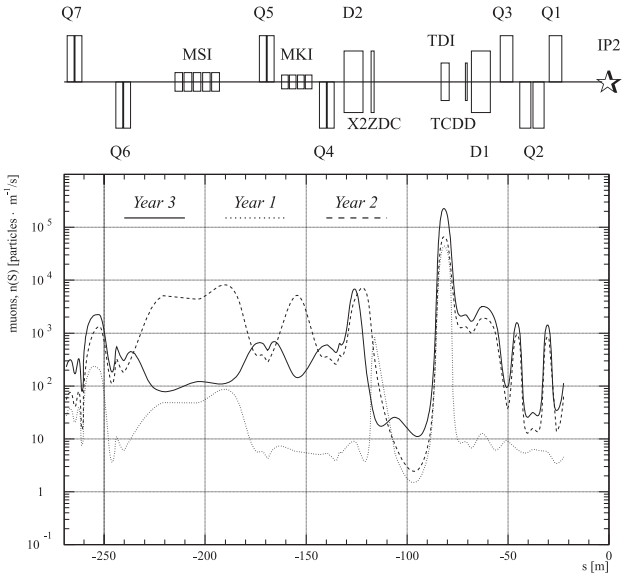

Figure 2: Number of muons as a function of primary proton-nucleus interaction distance to IP2.

plane, located close to the IP, where the trajectory of each particle was cut and particle characteristics were recorded. These characteristics included particle kinetic energy, direction cosines and coordinates of particle track crossing the scoring plane. In order to be able to provide the subsequent reconstruction of secondary particle fields in the presence of the residual gas density distribution, each particle track was tagged with the distance to the interaction from the point of the primary proton–nucleus collision, and the type of the residual gas nucleus, with which the interaction occurred. In addition, for each particle which fell into the recorded source, the coordinates of the hadron–nucleus interaction point were kept, where this particular hadron was born, or, for muons, the parent pion. This made it possible to trace back the history of the background particles and not only to study the contribution to the machine induced background from different parts of the insertion region, but also to spot the sections where most of the secondary particles that reach the experimental zone escape from the structure of the machine.

5 SECONDARY PARTICLE FLUXES

The results of the simulations, folded with the gas density profiles, are presented in Figures 1–4, for the three scenarios of the LHC operation [8] — a basic one, "3rd year +90 days", labeled *Year 3*, and for two other cases, "1st year after 70 days" and "2nd year +10 days", labeled *Year 1* and *Year 2* respectively. At the top of each figure a sketch of the corresponding machine structure is given, which includes all the major elements of the straight section.

The first two figures give the number of hadrons and muons in the insertion region, as a function of the primary proton–nucleus interaction distance to the interaction point. The values of secondary flux eg. for muons can be obtained by integrating the given distributions along the S axis. This gives the value of 1.03×10^6 muons/s for the muon flux under the "3rd year +90 days" LHC running conditions, and the values of 0.17×10^6 and 0.75×10^6 muons/s, for the "1st year after 70 days" and "2nd year +10 days" cases, respectively. The relatively smaller values for the first two years of the accelerator run reflect the decreased value of the nominal current at that period, which is assumed to be 20 % in the first year, and 30 % in the second year of LHC operation. As for the values of the secondary hadron flux, they are about an order of magnitude higher than the corresponding muon flux values for all three cases.

In the basic case, after 90 days of LHC operation in the third year, about 80 % of the background appears to be induced by the beam–gas interactions in the region of the injection absorber TDI. Among the other auxiliary peaks in the gas density profiles, the most significant increases can be seen in the injection line magnets region for the case of the second year operation, but even there it does not exceed the effect of the peak in the TDI. Thus the region of the injection shielding is currently the most critical region of the straight section, because of the residual gas density.

6 BACKGROUND FORMATION

The results, presented in Figures 3 and 4, show the secondary fluxes in the insertion region from a different point of view. These two figures give the number of hadrons and muons as a function of the distance to the IP from the point of the hadron–nucleus interaction, where a particular hadron was born, or, for muons, from the origin of the parent pion. Since these distributions are obtained using the same normalization, as those in Figures 1 and 2, they present the same integral values for the secondary fluxes, but distributed in a different way along the S axis of the

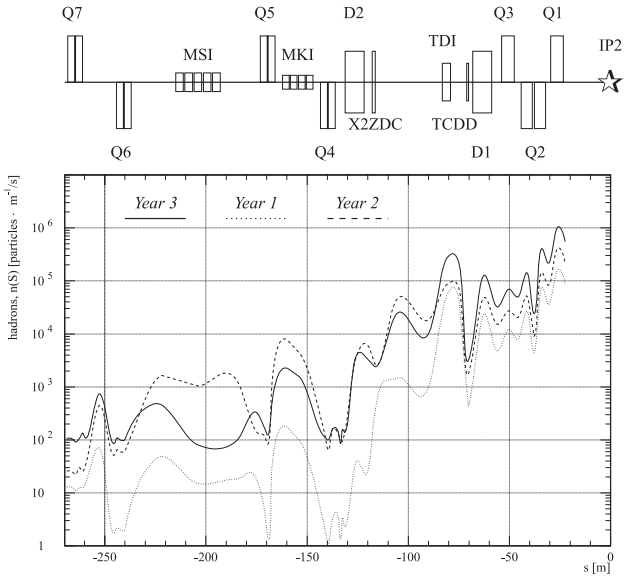

Figure 3: Number of hadrons as a function of last proton-nucleus interaction distance to IP2.

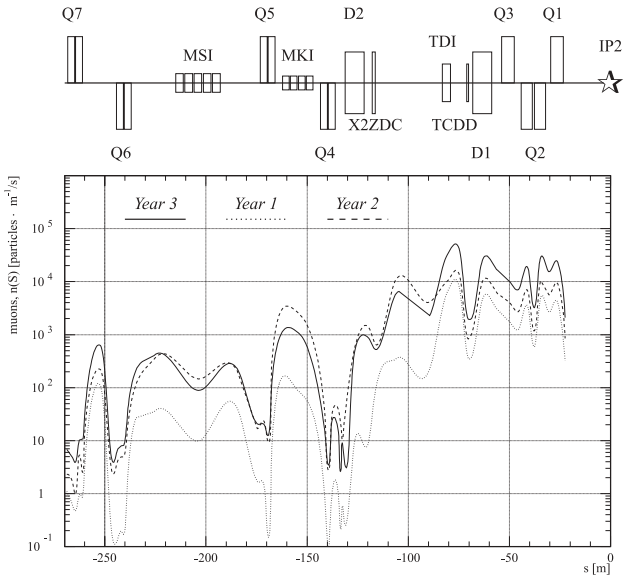

Figure 4: Number of muons as a function of last proton-nucleus interaction distance to IP2.

straight section. So by their definition Figures 3 and 4 show the sections of the machine structure, where the actual background particles, rather than their ancestors, are produced.

The distributions of hadrons in Fig. 3 demonstrate that the particles that interact with the nuclei of the residual gas, for example, around the TDI, do not necessarily produce a secondary cascade, which will contribute to the background, in the region close to the point of the primary interaction. The distributions still have distinct peaks in the position of the TDI, formed by the particles, escaping directly from the TDI–D1 drift space. But in the new representation this peak is now followed by a further increase along the inner triplet, illustrating the previously discussed "bottleneck" effect [3]. Generally for all three profiles of the gas density, the closer to the scoring plane the region of the last interaction, the more secondary hadrons are collected from it. In the muon distributions, the contribution of the D2–Q1 section is almost constant, with peaks in between the elements, where parent pions are not stopped by the material of the magnets.

7 CONCLUSION

The introduction of realistic profiles for the average residual gas density in the machine induced background simulations in the low luminosity insertion regions enables the estimation of contributions of secondary particle fluxes from the different parts of the straight section. The new estimates can be compared with the ones that were obtained for IR8 [6] and which were based on the previously published data on the residual gas composition. This comparison shows an increase by a factor of 5 in the secondary muon and hadron flux at the entrance to the experimental cavern. The increase for the scenarios of the long–term LHC operation is almost entirely due to the assumed very high residual gas density in the region of the TDI absorber.

8 REFERENCES

[1] I. Azhgirey *et al*. "Background muons generated in the CMS detector area by the beam losses in the LHC". In: One Day Workshop on LHC Backgrounds, CERN, Geneva, March 22, 1996.

[2] The LHC Study Group. "The Large Hadron Collider Conceptual Design". CERN-AC-95-05, Geneva, 1995.

[3] I. Baishev *et al*. "Proton losses upstream of IP8 of LHC". CERN LHC Project Report 500, Geneva, 2001.

[4] I.R. Collins and O.B. Malyshev. "Dynamic Gas Density in the LHC Interaction Regions 1&5 and 2&8 For Optics Version 6.3". CERN LHC Project Note 274, Geneva, 2001.

[5] A. Mathewson. "First Estimates of the Gas Density in the LHC Vacuum System". In: One Day Workshop on LHC Backgrounds, CERN, Geneva, March 22, 1996.

[6] I. Azhgirey *et al*. "Methodical study of the machine induced background in the IR8 of LHC". CERN LHC Project Note 258, Geneva, 2001.

[7] I. Azhgirey and V. Talanov. "The status of MARS program complex". In: Proc. of XVIII Workshop on the charged particles accelerators, Protvino, 2000, vol. 2, p. 184–187.

[8] I. Azhgirey *et al*. "Calculation of the machine induced background in the IR2 of LHC using new residual gas density distributions". CERN LHC Project Note 273, Geneva, 2001.